Institute of Parallel and Distributed Systems
University of Stuttgart
Universitätsstraße 38
D–70569 Stuttgart

Studienarbeit Nr. 2395

Investigation of Underwater Communication and Sensing by Means of Nonlinear Coupled Oscilators

Everardo González Ávalos

Course of Study:	Techinsche Kybernetik
Examiner:	Prof. Dr. rer. nat. habil. Paul Levi
Supervisor:	Dr. rer. nat. Serge Kernbach Dipl.-Ing. Tobias Dipper
Commenced:	11. 10. 2012
Completed:	11. 01. 2013
CR-Classification:	H.4.1, K.1

Abstract

This student thesis explores the relevant mechanisms that work behind underwater data transmission via potential fields and describes the first attempts to use this for achieving the coupling of two oscillators. It also describes a first approach to the implementation of a potential-field based control and localization of a group of autonomous underwater vehicles. An account of the different observations made and challenges faced is given.

Contents

List of Figures

1 Introduction

1.1 Localisation and Communication of Autonomous Underwater Vehicles

With oceans accounting for approximately 71% of our planet's surface, underwater exploration has always been an undertaking of enormous importance for the human kind. The richness of the waterbodies plays a very important role in many different fields, e.g. science (biology, geology, anthropology...)[1], [2], economy [3] and politics, and yet, it is only in recent times that technology has allowed to overcome many of the greatest challenges inherent to this activity. One of the major obstacles is the fact that the extreme conditions such as high pressures, low and high temperatures, and the lack of air to breathe, make this an exceptionally unsuitable environment for human life. It is progressively being tackled by the use of autonomous underwater vehicles (AUVs).

Traditional AUVs are big and costly platforms of difficult deployment. They usually consist of one single unit which is thereby highly susceptible to any malfunctions and whose failure often results in an enormous monetary loss [4]. Large groups of smaller AUVs which can collectively perform a given task with more efficiency and at a lower cost per unit are therefore an appealing alternative [5].

While the underwater cooperative robotics is a promising field blooming innovation [9], swarming AUVs posse challenges of their own, localization and communication being some of the most meaningful.

1.1.1 Communication by Means of Underwater Acoustics and Blue Light

Underwater acoustics and blue light are currently two mediums for wireless underwater communication and localization of great importance.

The high propagation speed of sound in water (about 1500m/s), high propagation range for low frequencies, and the mechanisms of acoustics which are easily grasped by human beings, have led to a widespread use of this medium for underwater communication. In the AUV field, acoustics are a highly valued and well studied way of communication ([6],[7]). On the downside, the speed of acoustic waves in water is highly dependent on many factors like temperature, pressure, and salinity. With this, the propagation range and direction are affected by any variation of the above mentioned parameters. The propagation range is also dependent on the signal frequency which forces a compromise between data ratee (higher for high frequencies) and propagation distance (higher for low frequencies).

Traveling at speed of light, electromagnetic waves are not only considerably faster than acoustic waves, but also impervious to temperature, salinity and pressure changes in water. Alas they are strongly attenuated in this medium and, depending on the medium, their propagation distance can be extremely low ([8]).

1.1.2 Underwater Electric Communication and Localization

Instead of yielding to other methods that are more intuitive for earthbound creatures, state of the art solutions take advantage of the conductive properties of water including use of electrical fields. Often found to work effectively in nature [10] [11], the underwater communication and localisation via electric fields has remained relatively unexplored in the AUV field. Nevertheless this method provides an attractive alternative that deserves a better exploration.

1.2 Goals

The objective of this work is to achieve a better understanding of the different phenomena involved in underwater-electrical-fields communication. Through practical experimentation rather than theoretical research, an insight into the strategies needed for the implementation in the control and localization of an AUV swarm is to be gained.

The totality of this work comprehends the following tasks:

- Creation of a pair of electric probes that fulfill the minimum hardware requirements to establish communication. This is, that are able to send and receive signals in the form of underwater electrical fields.
- Selection of a suitable test signal; a difference equation that is capable of coupled, stable oscillation.
- Identification of the influence of water's damping properties on the electric potential fields, particularly regarding the variation of distance in the range of what could be a reasonable interaction radius for the AUVs presented in 1.3.
- Analyzing the role own signals play in the sensorial perception and developing a method for the probes to filter them out in their measurements.
- The embodied coupling of the signals emitted by two different probes to achieve stable oscillations.

1.3 Related Work

1.3.1 ANGELS

ANGELS ("**Ang**uilliform Robot with **El**ectric **S**ense") is an interdisciplinary Europe-wide research project whose aim is to create a reconfigurable swarm of underwater robots with electric sensing, that are able to swim as single individuals, or, cooperatively emulate the movement of anguilliform fish. In each case, electric sensing will be used to achieve both, localization of single individuals and communication among them. Such robotic systems are intended to perform under circumstances adverse to visiual communication and classic propulsion systems.

> "The aim of the ANGELS project is to investigate interactions between body morphology and behaviour by designing and building a prototype for a reconfigurable anguilliform swimming robotic system. The robot will be able to function either as an eel-like whole entity, or may split into smaller agents (and vice-versa). These two different morphological forms will use a bio-inspired "electric sense", both for recognition of objects and obstacles, and for communication between agents, and will explore and exploit the different swimming and electro-sensing strategies used by gymnotid and mormyrid electric fish. Such a robotic system is intended to be used for recognition of objects in environments where vision -for perception- and propellers -for locomotion- are not suitable due to murky water, industrial waste, sea weeds, etc." [13]

1.3.2 CoCoRo

The CoCoRo (Collective Cognitive Robots) project is a joint effort of 5 european universities whose aim is to create a swarm of autonomous underwater robots which is capable of dealing with a large variety of tasks in a collective-cognitive manner:

> "The CoCoRo project aims to create an autonomous swarm of interacting, cognitive robots. CoCoRo will develop a swarm of autonomous underwater vehicles (AUVs) that are able to interact with each other and which can balance tasks. Focal tasks of the CoCoRo-swarms are: ecological monitoring, searching, maintaining, exploring and harvesting resources in underwater habitats." [14]

2 Theory

2.1 Coupled Oscilators

A mathematical sequence that defines itself recursively with the form

$$\overrightarrow{x}_{n+1} = \overrightarrow{f}(\overrightarrow{x_n}, \{\sigma\}),$$

with a state variable vector $\overrightarrow{x_n} \in \mathbb{R}^N$, a parameter set $\{\sigma\}$ and $n \in \mathbb{N}^+$, is called a map ([16]). Maps are discrete-time dynamical systems. The concept of stability[1] in this systems is of special interest. To study the stability of a system, the jaccobian matrix of the system

$$D_{\overrightarrow{x}_n} \overrightarrow{f}(\overrightarrow{x_n}) = \begin{pmatrix} \frac{\partial f_(x_1)}{\partial x_1} & \dots & \frac{\partial f_(x_1)}{\partial x_N} \\ \dots & & \dots \\ \frac{\partial f_(x_N)}{\partial x_1} & \dots & \frac{\partial f_(x_N)}{\partial x_N} \end{pmatrix}, \tag{2.1}$$

is calculated. The eigenvalues λ of the jaccobian matrix, are calculated by solving the foliowing equation:

$$det \| D_{\overrightarrow{x}_n} \overrightarrow{f}(\overrightarrow{x_n}) - \lambda I \| = 0. \tag{2.2}$$

Evaluating this eigenvalues at the fix points $\overrightarrow{x}_{n+1} = \overrightarrow{x_n}$ will return a concrete value for λ. A time-discrete dynamical system is stable and will thus converge if $\|Re\{\lambda\}\| < 1$ ([15]). If $\|Re\{\lambda\}\| > 1$ then the system is unstable and it will diverge to $+\infty$ or $-\infty$.

A map with orbits [2] that fail to converge, without diverging to $+\infty$ or $-\infty$, can be called an oscillator ([15]) (Fig.2.1).

[1] The concept of stability is a delicate one; the definition used in this work can be found in [15] and [17]

[2] the sequence $O = \{\overrightarrow{x_n} | \overrightarrow{x}_{n+1} = \overrightarrow{f}(\overrightarrow{x_n}), n \in \mathbb{N}_0^+\}$ ([16])

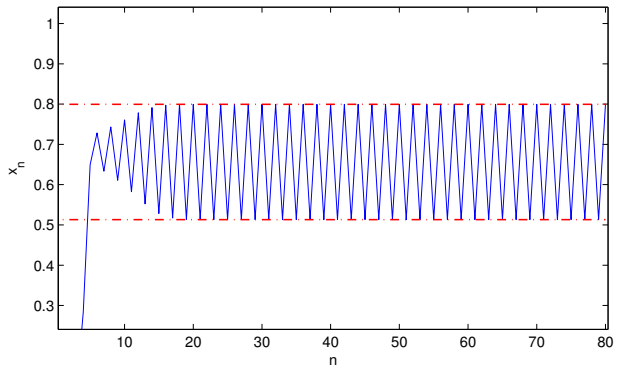

Figure 2.1: The equation $x_{n+1} = \alpha x_n(1 - x_n), \alpha = 3.2$, also known as the logistic map [16], oscillating between it's upper and lower limits (red pointed lines).

2.2 The Logistic Map

The logistic map

$$x_{n+1} = \alpha x_n(1 - x_n) \tag{2.3}$$

with it's control variable α, is a time-discrete dynamical system with the fix points

$$x_1^* = 0 \text{ and } x_2^* = 1 - \frac{1}{\alpha}.$$

After calculating the jaccobian matrix (equation 2.1), the eigenvalues for this two fix points reveal themselves as

$$\lambda_1 = |\alpha| \text{ and } \lambda_2 = |2 - \alpha|.$$

According to equation 2.2 the fix points are only stable for the α intervals $[0, 1]$ and $[1, 3]$ respectively. And yet increasing the value of α over this bound does not show an unstable orbit, but rather one with oscillating solutions (Fig.2.2).

The range $\alpha > 3$ for example, shows a periodic repetition of two values. Mathematically speaking this means $x_{n+2} = x_n$, this expression can be transformed in the following way

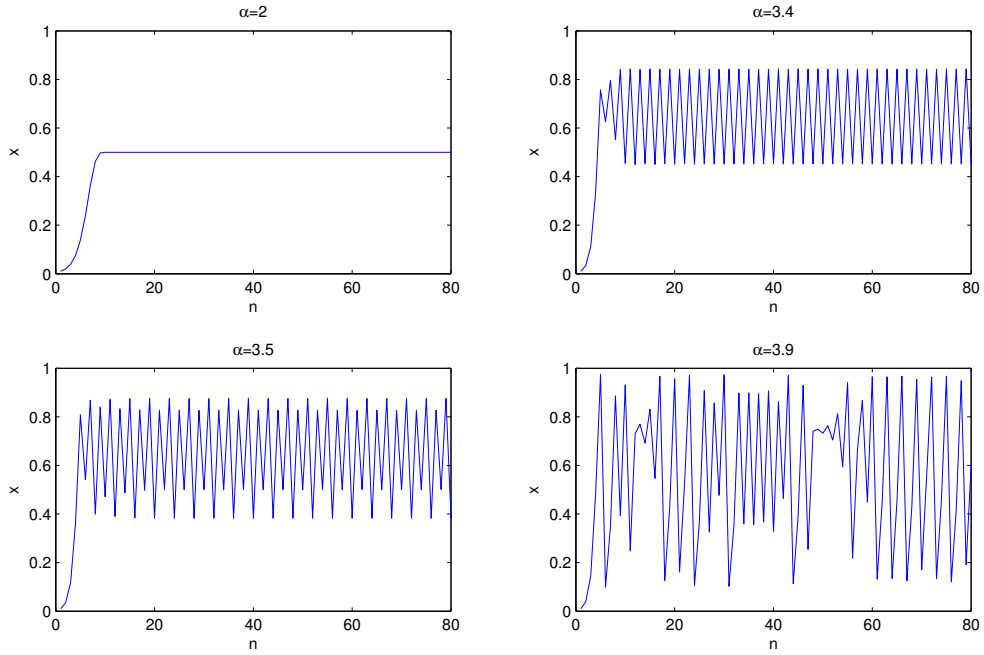

Figure 2.2: Plots of the logistic map with different α values.

$$\begin{aligned} x_{n+2} &= f(x_{n+1}) \\ &= f(f(x_n)) \\ &= \alpha(\alpha x_n(1-x_n))(1-(\alpha x_n(1-x_n))) \\ &= \alpha^2(\alpha x^2(x^2-2)+x(1-x)). \end{aligned}$$

The stability analysis for the fix points of this new equation reveals stability for the α interval of $[3, 1+\sqrt{6}]$. This is on par with the 2-period oscillations range of α in equation 2.3 . As the value for control parameter α increases, the logistic map will keep on exhibiting interesting dynamics of this kind. A more practical way to explore this behaviour is plotting the final result of a long line of iterations of $f(x_n)$ as a function of the varying control parameter α. The resulting diagram is called a bifurcation diagram ([16]) (Fig.2.3).

2.3 Electric Fields

Parting from the definition of an electric field **E** as the force **F** per unit charge q acting at a given point ([19]):

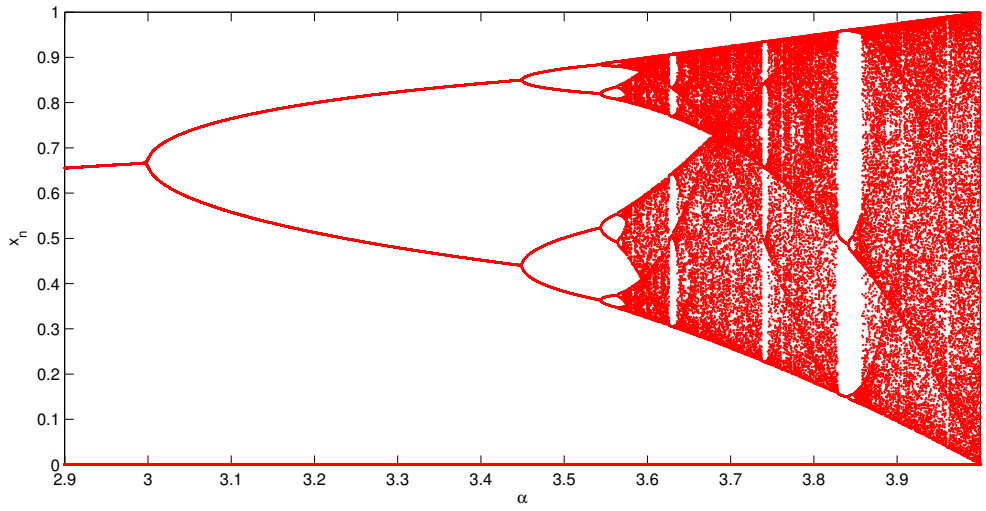

Figure 2.3: Bifurcation diagram of logistic map (eq.2.3) with different α values between 2.9 and 4

$$\mathbf{E} = \frac{\mathbf{F}}{q}, \tag{2.4}$$

and using Coloumb's Law

$$\mathbf{F} = kq_1q_2\frac{(\mathbf{x_1} - \mathbf{x_2})}{|\mathbf{x_1} - \mathbf{x_2}|^3}$$

where k is a constant of proportionality, q_1 and q_2 are two point charges in $\mathbf{x}_1$ and $\mathbf{x}_2$, and $\mathbf{F}$ the resulting force in point $\mathbf{x}_1$, the electric field can be defined as a function in space:

$$\mathbf{E}(\mathbf{x}) = kq_1\frac{(\mathbf{x} - \mathbf{x_1})}{|\mathbf{x} - \mathbf{x_1}|^3}$$

The linear superposition of forces resulting from multiple point charges means our electric field can be expressed with a sum:

$$\mathbf{E}(\mathbf{x}) = k\sum_{i=1}^{n} q_i\frac{(\mathbf{x} - \mathbf{x_i})}{|\mathbf{x} - \mathbf{x_i}|^3}$$

or, if the charges are small and numerous enough, with the (three-dimentional volume) integral of the charge density $\rho(\mathbf{x}')$:

$$\mathbf{E}(\mathbf{x}) = k \int \rho(\mathbf{x}') \frac{(\mathbf{x} - \mathbf{x}')}{|\mathbf{x} - \mathbf{x}'|^3} d^3\mathbf{x}'. \tag{2.5}$$

(from [19])

Back to equation 2.4 and together with the definitions for work W as the product of the force $\mathbf{F}$ acting on a moving point $d\mathbf{s}$

$$dW = \mathbf{F} d\mathbf{s}$$

and voltage U as this work in relation to a charge q

$$U = \frac{W}{q},$$

the following relationship between voltage and electric fields can be established:

$$U = \int \mathbf{E} d\mathbf{s}. \tag{2.6}$$

Equations 2.5 and 2.6 expose two characteristics of electric fields relevant to this work: they relate directly to the voltage difference between two points, and do so in a linear manner, this is with homogeneity and superposition properties.

3 Methods

3.1 Experimental Setup

3.1.1 Hardware

The hardware developed and used for the experiments consists of two simple electrical probes as shown in Fig. 3.1. These probes have two tasks: the emitting and the receiving of underwater electrical potential fields. They consist each of a 15cm plexiglas pipe with four electrodes attached to it. The outer pair of electrodes is used as an emitter and the inner pair as a receiver. The four electrodes are connected to an electronic board containing an analog filter, an amplifier, a DAC and an ADC. This board is in turn connected to a PSoC5 micro-controller [20] via an SPI bus for data processing. The PSoC micro-controller can then be accessed by a PC via mini USB port and UART.

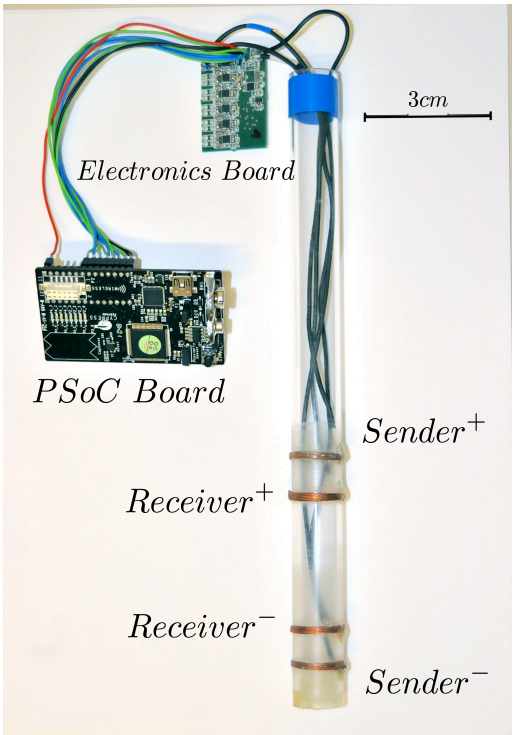

Figure 3.1: Electrical Probe consisting of two pair of electrodes, an electronic board and a PSoC micro-controller.

The voltage between the emitting electrodes is directly controlled by a 12-bit DAC (AD5322) which can independently generate an analog voltage between 0V and 5V for each output. This corresponds to a relative voltage of ±5V between the electrodes. Due to the high damping qualities of water, the potential field caused by this voltage difference will only generate an input for the receiver electrodes in the mV range; the measuring is therefore easily disrupted by noise and specially susceptible to constant electrical fields. Thus the necessity of two electronic components which are integrated in the electronics board. First, a high-pass filter with the cut-off frequency of less than 16Hz made out of a capacitor and a resistor (Fig. 3.2), connected directly to the receiving electrodes. The second component is an operational amplifier (AD8226) with a gain of 500. Because of the ±5V input, this gain enables the reading of voltages in the ±10mV range.

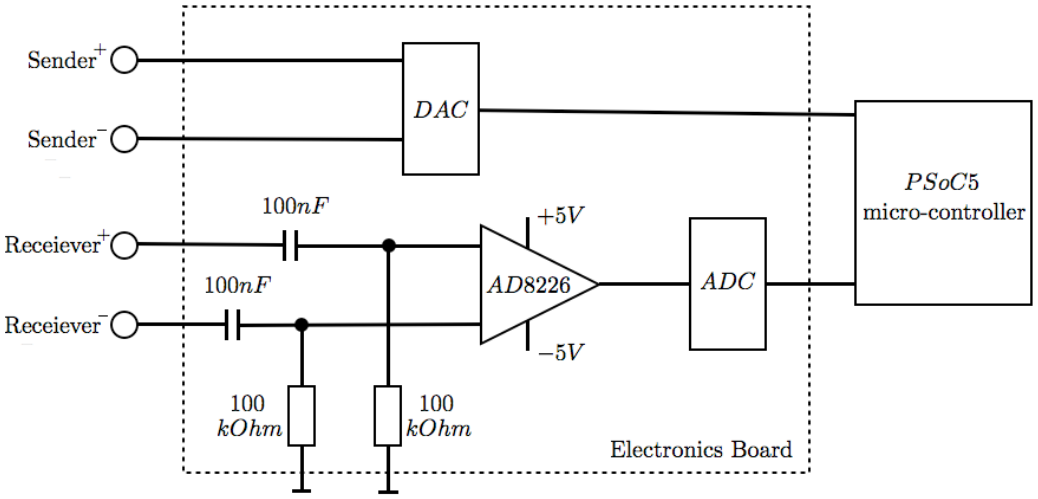

Figure 3.2: Schematic of the electronics board.

The electrical probes were mounted on a longish piece of plastic, in a manner such that the distance between them can be varied while remaining parallel to each other. All experiments took place in a large aquarium at a depth of 2.5cm for the first electrode and 10cm for the last one (Fig. 3.3a). To avoid external signal disturbances and artifacts, each probe was connected to a laptop computer running on battery, all other sources of electronic noise were either removed or shut down and the water in the aquarium was earthed (Fig. 3.3b).

3.1.2 Software

The software implementation of this work is divided in two main sections: the programming of the microprocessor and the processing of the received data. While the second task could

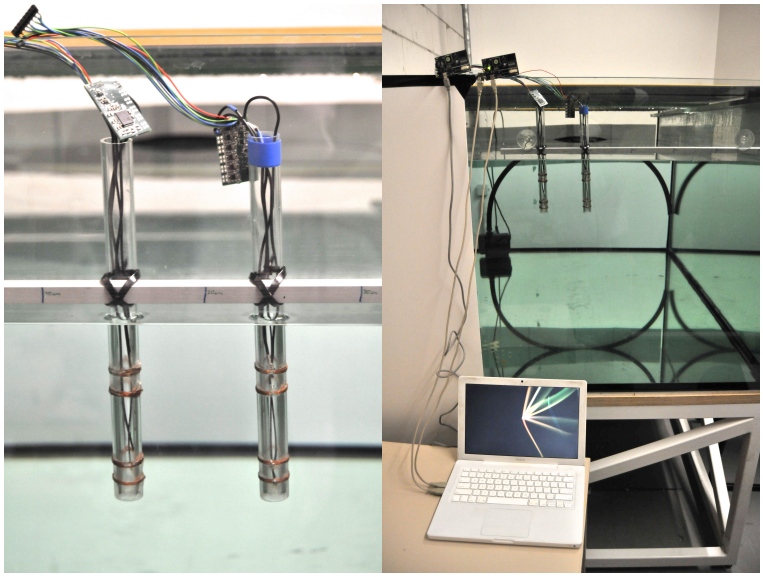

(a) **(b)**

Figure 3.3: Two mounted probes **(a)** and the complete experiment environment **(b)**

easily be merged into the first one, we made use of different software tools and programming languages better fitting for the one or the other, thus the importance of telling them apart, even though this differentiation is not of much importance for the final result.

Microprocessor Programming

The programming of the used PSoC5 microprossesors takes place with the PSoC Creator IDE [21]: a hardware/software co-design environment which allows the custom configuration of the integrated analog and digital peripherals in the PSoC5 boards as well as a C-based development flow. The software running on the microprocessor is responsible of initializing the system and the equation, iterating the equation, writing the output data in the DAC, and reading the input data from the ADC, following the sequence shown in Fig.3.4.

Data Processing

While some tasks of the data processing are simple and could be easily integrated to the microprocessor routine, the manipulation required for other processes deemed worthy of more specialized tools. In this case the data read from the ADC was sent to the PC via a UART Serial and loaded with MatLab [22] and saved as a corresponding file for further analysis. Disregarding the various functions regarding, the initialization the GUI, and the UART connection, the basic main loop can be described as follows:

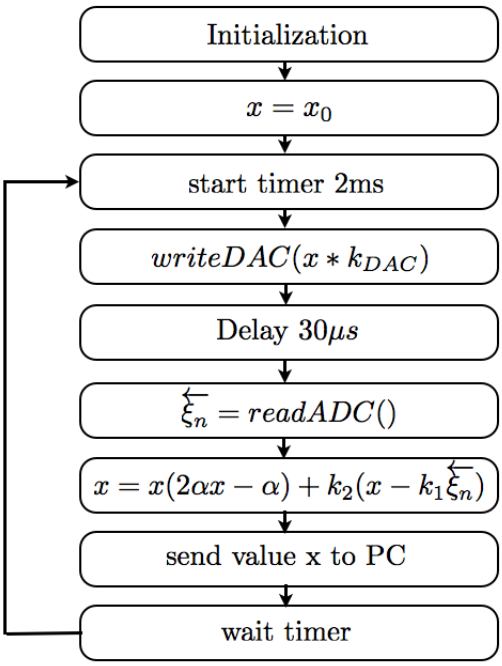

Figure 3.4: Flowchart of the algorithm running on the PSoC5 Boards.

In the first step the binary writing of a value into the microprocessor triggers the program running on it (Fig.3.4)

```
28
% Sync ausloesen
30 fwrite(s, number);
fwrite(s, get(handles.popupmenu_filter, 'Value')+9);
```

The loop starts with the reading of one out of 1000 values from the UART.

```
32 while(run)
    tic;
34
    % Aktueller Wert erhoehen;
36  if wert>=1000
        wert = 1;
38  else
        wert = wert + 1;
40  end
```

```
42      % Messung abrufen
        wait_response(s,5,2);
44      uartdaten = fread(s,2, 'uint8');
```

After this follows the manipulation of the single information bits contained in this value, to create a decimal value out of it, and save it in an array. This is array represents the results of every iteration of the equations sent.

```
46      % Messung verarbeiten

48      daten(wert) = uartdaten(1)*256 + uartdaten(2);

50      if daten(wert)=<32767
              daten(wert)=daten(wert)/40000; % 40000 is the amplification factor from electronics board
52      else
            daten(wert) = 65536 - daten(wert);
54          daten(wert)=-daten(wert)/40000;
        end
```

The final step is displays the data in the GUI and waits for a timer to restart the loop.

```
58      % Plot darstellen
        if mod(wert,20)==0
60          set(p,'Ydata', daten);
            set(handles.text_app, 'string', ['Ap-p: ' num2str(max(daten)-min(daten), '%1.3f') 'V']);
62          set(handles.text_mean, 'string', ['Mean: ' num2str(mean(daten), '%1.3f') 'V']);
            pause(0.0001);
64      end
       % disp(toc)
66      while (toc < 0.001)
            pause(0.00001);
68      end
end
```

Once the data is obtained in this way, it can be saved for further analysis or manipulated to other ends.

3.2 Used Equations

In order to achieve a better understanding of the underwater potential fields in this specific application, two different, non linear, time discrete dynamical systems are used. These are not only well suited for the implementation in the micro-controller but also widely studied ([18]) and posses a solid theoretical frame around them that allows a proper analysis ([17]), and are

therefore optimal candidates to explore quantitative and qualitative changes concerning their orbits.

Starting with the logistic map (equation 2.3). The behaviour of this equation discussed in section 2.2, specially the one regarding stability, the periodic and chaotic trajectories, and the bifurcation points, are interesting characteristics because they are specially susceptible to any alterations.

The only unfavorable quality of equation 2.3 are the non-zero constant solutions for $\alpha \in [1, 3]$. These constant solutions are suppressed by a high-pass filter described in 3.1.1. In order to acquire a transformation of the logistic map without this constant potential, the non-periodic stationary states are removed as in [12], by solving $x_n = \alpha x_n(1 - x_n)$ to $x_{st_1} = 0$ and $x_{st_2} = \frac{a-1}{a}$ with stable regions in $\alpha \in [-1, 1]$ and $\alpha \in [1, 3]$ respectively. After the substitutions $y_n = x_n + \frac{\alpha-1}{\alpha}$ and $y_{n+1} = x_{n+1} + \frac{\alpha-1}{\alpha}$ and solving the system for x_{n+1} the foliowing equation is obtained:

$$x_{n+1} = x_n(2 - \alpha x_n - \alpha). \tag{3.1}$$

In Fig.3.5 the bifurcation diagrams of both equations are plotted. The new system is free of non-zero constant solutions but nevertheless retains the main characteristics of 2.3. A further favorable quality of this system is the continuos oscillation between positive and negative values. This makes it possible to fit the signal to the emission window (±5V) without the need of an offset value.

3.3 Embodied Coupling

The coupling of multiple equations like the one described in section 3.2 leads to a system with the form

$$x_{i\ n+1} = f[x_{i\ n}] + \sum_{j \neq i} f[x_{j\ n}]$$

and the number of coupled equations $i = j$. While future applications of this communication method consider a large number of agents and therefore a large number of coupled equations, the experiments in this work will be of the simplest, kind incorporating only two elements:

$$\begin{aligned} x_{1\ n+1} &= f[x_{1\ n}] + f[x_{2\ n}], \\ x_{2\ n+1} &= f[x_{2\ n}] + f[x_{1\ n}]. \end{aligned}$$

The main part of the coupling embodiment takes place underwater. The difference equations are computed in a micro-controller, and every result x_{n+1} of each iteration n is converted to an analog signal $\overrightarrow{\xi_n}$ which is then sent underwater. The coupling takes place when the water signal $\overleftarrow{\xi_n}$, containing fractions k_1 of the foreign and the own signal $\overrightarrow{\xi_n}$, is read and taken

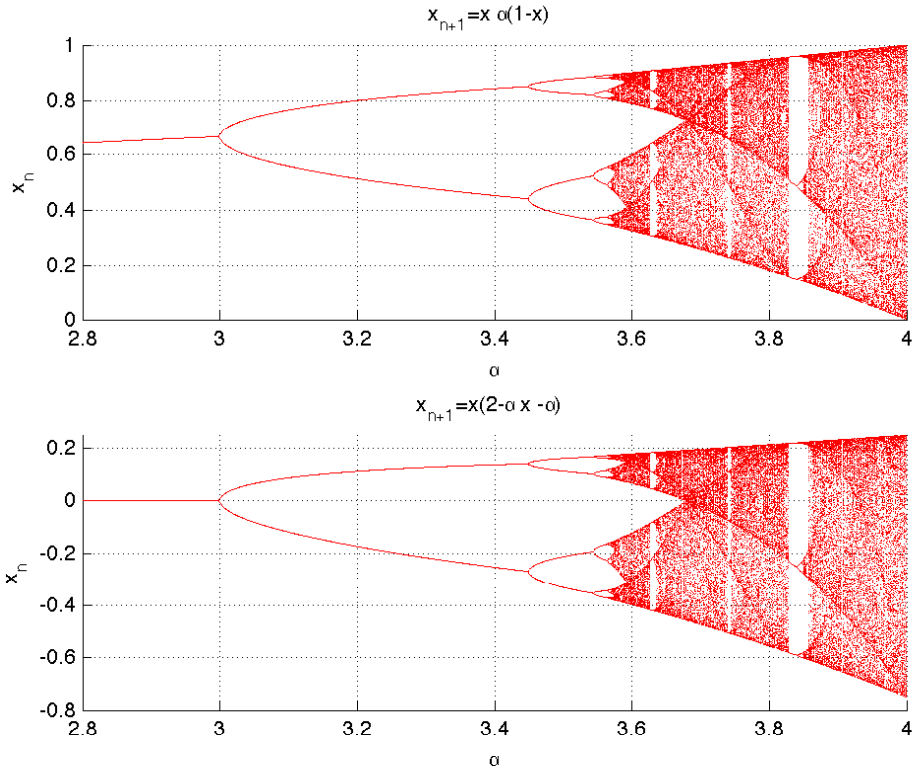

Figure 3.5: Bifurcation diagrams of the logistic map and the new transformed equation.

into consideration to compute the next step of the difference equation. With this physical embodiment, each equation in the system takes the following form:

$$x_{n+1} = f[x_n, \alpha] + k_2 \overleftarrow{\xi_n}$$

with the amplification factor k_2.

An important part of the coupling experiments relies on eliminating the fractions k_1 of the own signal $\overrightarrow{\xi_n}$ from $\overleftarrow{\xi_n}$ and reading only the signals from other oscillators (see Fig.3.6). By doing so, following system is obtained:

$$\begin{aligned} x_{n+1} &= f[x_n, \alpha] + k_2(\overleftarrow{\xi_n} - k_1 \overrightarrow{\xi_n}) \\ \overrightarrow{\xi_n} &= x_{n+1} \end{aligned} \tag{3.2}$$

Equation 3.2 with its two coefficients k_1 and k_2 is the final system running on each oscillator (Fig.3.6).

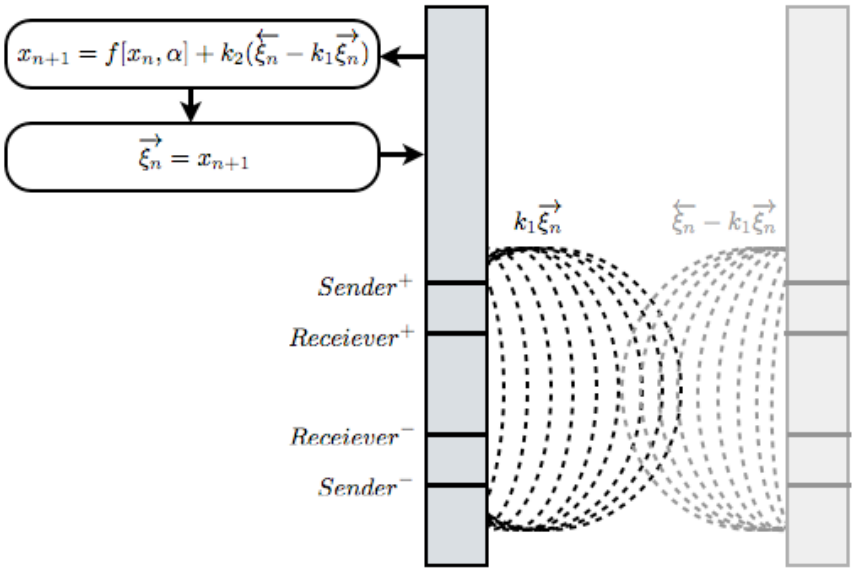

Figure 3.6: Schematics of the embodied coupling.

4 Experiments

The final goal of coupling the potential-field oscillators was approached systematically through three different experiments. In 4.1 the objects of study are the signal strength and it's variation with the distance of emitting and receiving probes and the proximity to objects. In 4.2 the coefficient $k1$ from 3.2 is calculated so that the system of coupled equations can be studied in 4.3.

4.1 Dependency Between Signals

In this first experiment, the investigation of the behavior of the underwater signals takes place in a straightforward practical manner. While the mechanisms that take place in underwater electrical fields are well known ([19]), the theory of fields is difficult to apply in a practical environment where many parameters are beyond one's control. Thus the importance of experimental observation to back up the theory and aid the comprehension of phenomena involved in all further experiments.

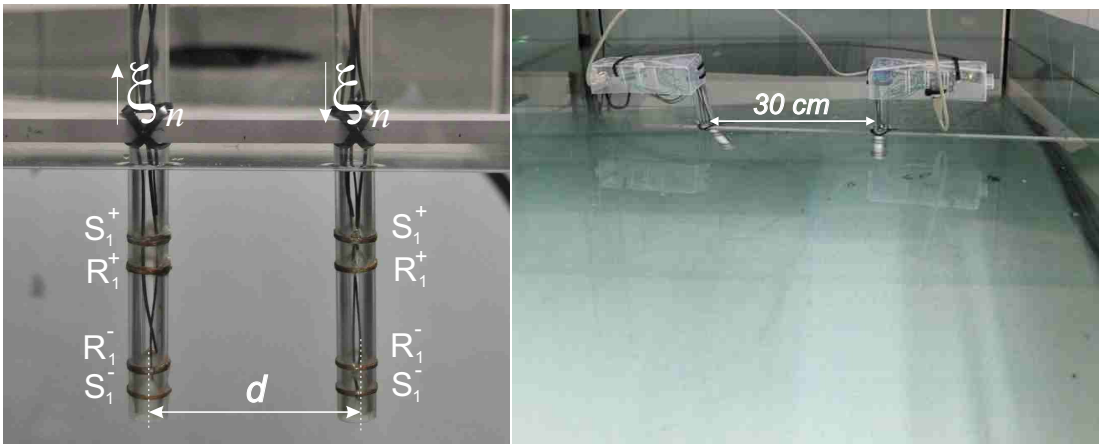

(a) **(b)**

Figure 4.1: Two probes with a distance d right next to the wall (4.1a) and in the middle of the tank(4.1b).

The effects that two different variables have on the signal strength are studied, specially its increase or decrease depending on the distance between the emitter and receiver as well as the proximity to other objects i.e. the aquarium walls. To do so an electrical probe as emitter

and a second one as receiver (Fig.4.1a) are used to measure the perceived amplitude of initial 80 iteration steps of equation3.1: first with a periodic signal (coefficient $\alpha = 3.1$) and then a chaotic one (coefficient $\alpha = 3.7$). The distance varied from 2.5cm to 30cm in intervals of 2.5cm. This measurements were made mounting the probes directly against the wall; for the periodic signal the measuring is repeated, mounting the probes in the middle of a 200cm$x$140cm$x$65cm tank (Fig.4.1b). The evaluation of the results was a direct comparison of the measurements, taking the strongest possible signal, the signal produced by the measuring probe itself [1], as a standard to compare the rest of the signals from higher distances.

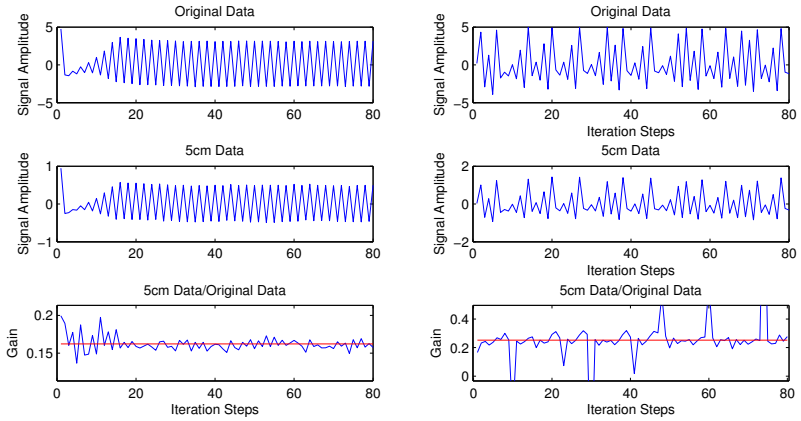

Figure 4.2: The comparison of the original (0cm) signal and a signal taken with a distance of 5cm for an equation with periodic (left) and chaotic (right) results, and their respective gain (mean gain in red).

By dividing the measured signal strength by the respective values of the 0cm signal a gain suitable to express the strength decay that comes with an increasing distance is obtained.

Distance [cm]	5	7.5	10	12.5
Mean gain for $\alpha = 3.1$	0.1603	0.0783	0.0423	0.0255
Mean gain for $\alpha = 3.7$	0.2500	0.1270	0.0601	0.0346

Table 4.1: Mean gain measures for the distances between 5cm and 12.5cm for a periodic ($\alpha = 3.1$) and a chaotic ($\alpha = 3.7$) signal.

Plotted with its confidence intervals of 95%, the relationship between signal strength and distance reveals itself as nearly-linear for the relevant distance interval between 2.5cm and 12.5cm (Fig.4.3). While the chaotic signals show a lesser strength decay (most certainly because of their bigger amplitude), the dynamics of the chaotic mode are extremely sensitive to disturbances which shows in the big confidence intervals. The behaviour of the periodic mode is highly stable and it's signal strength is well reliable until passed the 20cm without being compromised by the measured noise.

[1] This signal is also referred as the 0cm distance signal.

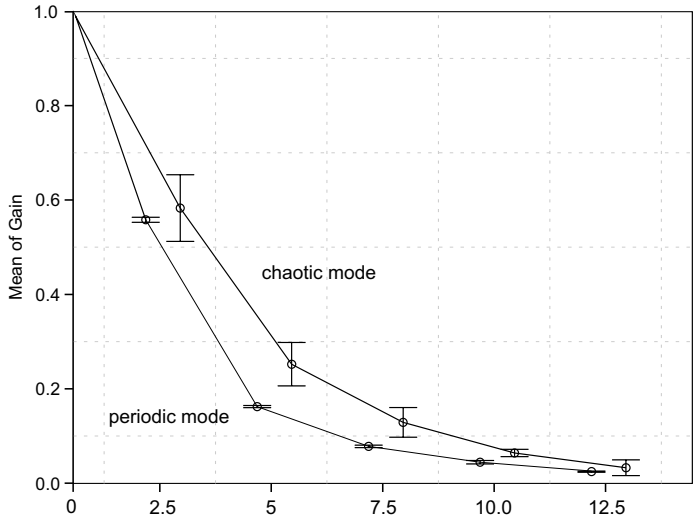

Figure 4.3: Mean gain measurements with a 95% confidence interval for both, chaotic and periodic signals.

The second measurements were made with the same parameters varying only the location of the probes which were now placed in the middle of the tank. An equation with periodic solutions ($\alpha = 3.1$) was used and, as before, only the first 80 iteration were used in the experiment. This resulted in a difference of importance regarding the amplitude of the measured signals, which is best described in table 4.2. Here the same method used to compare the signals in the first section of this experiment is used on the two different positions and in turn with each other.

Distance in cm	5	7.5	10	12.5
Mean gain for the tank-wand position	0.1603	0.0783	0.0423	0.0255
Mean gain for the tank-middle position	0.0739	0.0482	0.0304	0.0147
Relative gain	0.4610	0.6161	0.7196	0.5775

Table 4.2: Mean gain measures for the distances between 2.5cm and 12.5cm using a periodic ($\alpha = 3.1$) signal, for the probes placed against the tank wand and in the middle of it.

As expected, by varying the distance of the electrical probes to the aquarium wand a quantitative alteration of the signal was achieved, which in this case is expressed by an amplitude reduction. Since the difference in the distance to the aquarium glass borders remains constant for both measurements, one could expect a constant decrease of amplitude for varying probe distances. However, as shown in Fig.4.4, this is not the case, leading to the conclusion that whatever capacitive effects take place in the presence of a conductive or non conductive object, are not only affected by the distance to the object, but also by the strength of the potential fields themselves.

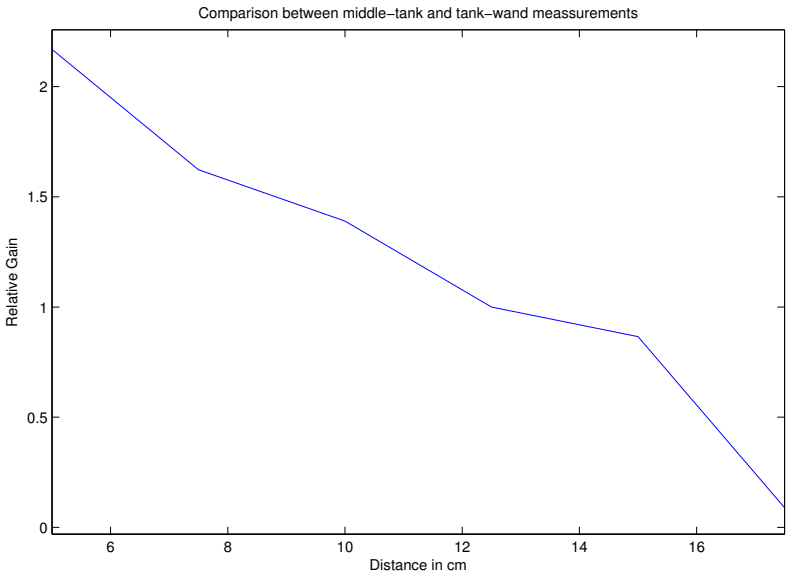

Figure 4.4: The strength decrease expressed as the mean signal strength of the measures made in the middle of the tank divided by the ones made at the wall.

4.2 Coefficient Calibration

The second experiment seeks to calibrate the coefficient $k1$ from the signal $\overrightarrow{\xi_n}$ emitted by the measuring probe itself as shown in equation 3.2 in order to eliminate all influence of the own signals in the reading of external ones.

The first step is to find an amplification factor for the output signal produced by the DAC, k_{DAC}. The main criterium for this factor is that the transmission range presented in section 3.1.1 is sized entirely but without over-saturating. As described in that section, this means, varying in between a maximum and a minimum value approaching $\pm 5V$ respectively. Various different values k_{DAC} depending on the amplitude of the original signal were calculated by reading the signal amplitude directly out of the emitters with an oscilloscope (Fig. 4.5). Since the amplitude of the signal varies drastically for $3.0 < \alpha < 4.0$ a compromise between a useful range for the oscillating results around $\alpha = 3.1$ and the over-saturation of the peaks in the chaotic results near the end of the spectrum has to be made. After determining a good sensing ability in 4.1, a factor $k_{DAC} = 2000 * 0.175$ was chosen for the rest of the experiments; the signals for the lower α range retain a satisfying definition while the integrity of the higher-amplitude chaotic signals is not compromised.

Determining the amplification factor k_{DAC} and thus the input of the system allows to reproduce a simplified, constant transfer function. To do this a test signal which oscillates between a positive and negative constant value is generated:

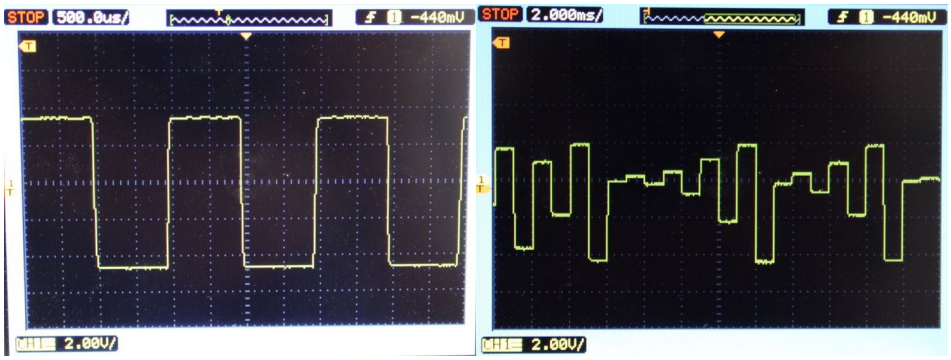

(a) **(b)**

Figure 4.5: Oscilloscope readings of the signals emitted by equation 3.1 with **(a)** $\alpha = 3.1$ and $k_{DAC} = 2000 * 6$ and **(b)** $\alpha = 3.7$ and $k_{DAC} = 2000 * 0.175$ *[from [12]].*

$$x[t] = \begin{cases} 1 & \text{if } t \in k * 100 + \{1...50\} \\ -1 & \text{if } t \in k * 100 + \{50...100\} \end{cases} \quad k \in \mathbb{N}. \tag{4.1}$$

The system response is then analysed (Fig. 4.6). By comparing the direct signal amplitude as read in an oscilloscope with the signal response from the underwater probe, the factor $k1$ is calculated between 0.17 and $= 0.24$. Repeated manual calibrations revealed these coefficients are strongly dependent of the experiment and vary with even the most subtle changes of it. In further applications the coefficient $k1$ was therefore calibrated automatically with the initialization of the system by varying it until $f[x_n, \alpha] - k_1\overrightarrow{\xi_n} \approx 0$.

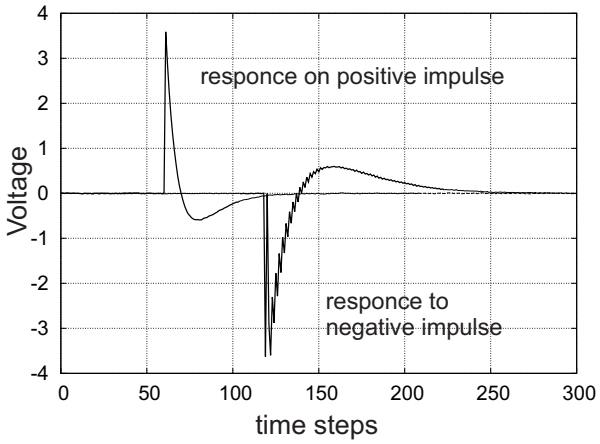

Figure 4.6: System response to the step function 4.1

The experimental setup to test this consisted of two probes both sending and receiving the results of the logistic map (Eq. 2.3) with a factor α in the range between 2.9 and 4.0, so as to

create a bifurcation diagram. The dynamics of such a system, specially the chaotic solutions, are delicate, and easily altered by disturbances, showing qualitatively and quantitatively changes. The system is therefore ideal to test the precision of our calibrated coefficient $k1$.

Comparing the ideal diagram (Fig. 4.7a) with the diagram generated by the same measuring probe (Fig. 4.7b) reveals quantitative and qualitative alterations. The quantitative alterations are dictated by different parameters like the factor k_{DAC} or the gain of the operational amplifier, and are therefore of less interest. Yet it is worth remarking the accuracy of k_{DAC} concerning the above mentioned saturation limit of $\pm 5V$. The qualitative changes, on the other hand, reveal an inverse sensing of the own signals (revealed in an inverted diagram). This is the result of inverted connection of the probes' electrodes. Using this valuable information a suitable coupling coefficient $k2 < 0$ is calculated and used to filter the own signals and reconstruct a satisfying bifurcation diagram out of the foreign probe emitted signals (Fig.4.7d). The results of this experiments attest the probes' capabilities to both, filter the own signals and read external ones accurately for all stable ranges of equation 3.1.

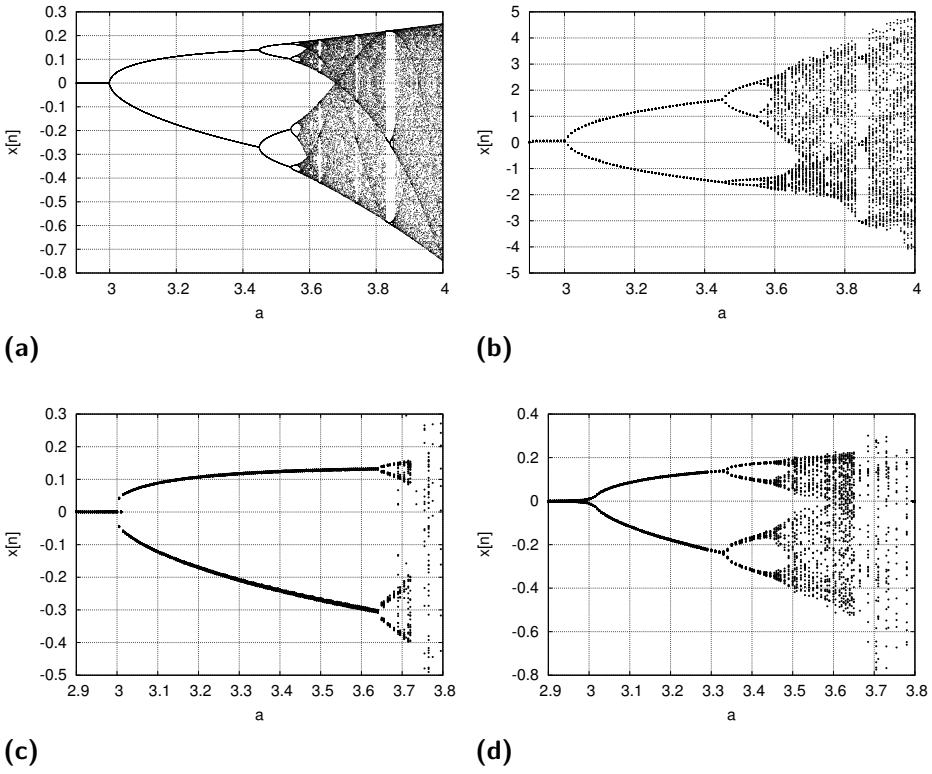

Figure 4.7: Bifurcation Diagrams of equation 3.2. Ideal Bifurcation Diagram **(a)**, real bifurcation diagram with $k2 = 0$ **(b)**, and a positive **(c)** and negative **(d)** coupling of a second probe ($k2 \neq 0$).

4.3 Potential-Field Coupled Oscillators

After exploring different qualities of the potential fields object of this study and calculating different parameters relevant to the mechanisms of communication, the final goal of this series of experiments, the embodied coupling of the oscillators, is addressed.

The setup for this experiment consists of the same two probes as in 4.2 which this time run equation 3.2. This means the expression $k_2(\overleftarrow{\xi_n} - k_1\overrightarrow{\xi_n})$, that, according to the results of 4.2, contains signals emitted by other foreign probes, is now part of the feedback loop creating a system of coupled oscillators with a behavior of it's own.

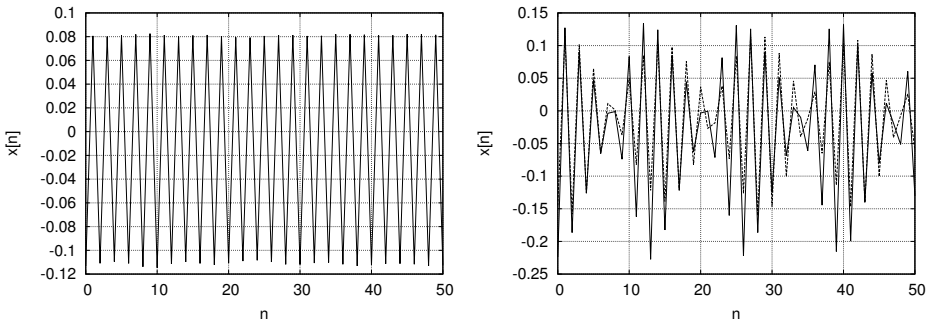

Figure 4.8: Results of equation 3.2 as in the underwater potential fields with **(a)** one emitting probe, and **(b)** two emitting probes.

In figure 4.8 a qualitative difference in the results of the experiments with one (4.8a) and two (4.8b) oscillators is seen. The different behavior of both systems attest for a successful coupling of the two emitted non-linear equation. This has many positive implications: among others, it gives account of the requirements for communication being completely fulfilled and the communication cycle taking place continuously and stably.

5 Discussion

This thesis explored the basic principles of underwater communication and localization using potential fields as can be applied in the context of a group of small AUVs like the ones proposed in [13], [14]. The evaluation of distance and precision in which this can be achieved were of special interest, as were the properties of water as a propagation medium.

The first step to achieve this was the creation of two underwater probes with a satisfying ability to create and measure underwater potential fields. The characteristics of these probes resembled the ones expected of compact AUVs. The adaption of said probes to other existent pieces of hardware such as the electronics board and micro-controller presented in the hardware section followed. Along with the matching software this builds an environment suitable for further related experiments.

Parting from the logistic map, an alternative chaotic equation was obtained through elimination of its non zero constant solutions. This new equation retains the main characteristics of the logistic map such as bifurcation points, peak-to-peak amplitude of the oscillating solutions, and chaotic behavior. The different experiments took advantage of these characteristics inherent to chaotic equations in order to prove underwater potential fields as a suitable form of communication and self localization for submarine devices in the germane size range.

In a first experiment the signal amplitude in relationship with the distance between the two probes was measured. The signal strength showed a close-to-proportional behavior, decreasing with growing distances. A range of at least 20cm revealed itself suitable for accurate transmission of information. Likewise, a significative difference in the amplitude of the signals measured in immediate proximity of the aquarium wand and the ones measured farther away from it, proved self-location by means of potential field to be possible.

After studying water damping effects, a set of parameters concerning the water qualities was calculated in the second series of experiments. This allowed each probe to tell apart the own emitted signals in the whole measurements of external signals. This strategy was used to filter the own signals and measuring exclusively foreign ones. The last experiment accomplished the underwater embodied coupling of two chaotic equations emitted by different probes. A new system that produced stable oscillations was achieved and proved continuos and accurate underwater communication via potential fields to be possible in our context.

While satisfactorily fulfilling the stablished goals, this work exposed new questions worth mentioning: The setup of this work was restrained to a system of two agents; in further works this should be expanded to larger groups of agents, aiming at the application of this results in the context of underwater-swarm-robotics. The use of potential fields as a way of detecting external objects was briefly proven as possible. Such an interesting possibility provided by

diverse electrical phenomena deems worthy of a deeper examination. The significance of the electromagnetic fields geometry is an aspect of high relevance that was not addressed in this work. The mechanisms involving non-linear chaotic equations proved a helpful ally in this first approach to the communication, and thus, the entire frame of this work renders exceptionally suitable to explore other exiting fields, synergetic- and self-organization-phenomena ([23]), being just one great example of this.

A Software Annexe

A.1 PSoC Software

```
2 */
#include <device.h>
4 #include <math.h>

6 #define BifurcationDiagram 0
#define CoupledOszilators 1
8
#define ActiveExperiment 2 // 0 - bif diagram; 1 - coupled osci; 2 - mirror
10
unsigned short pauseMainCLK;
12 unsigned short pauseSPIR;
unsigned short ustimer=0;
14 unsigned short pauseSPIS;
float  water_factor1, water_factor2;
16


18 /* Interrupt-Funktion Main-Clock */
CY_ISR(Interrupt_MainCLK){
20   Counter_MainCLK_ReadStatusRegister();
   pauseMainCLK = 0;
22   return;
}
24
/* Warten auf Main-CLK Interrupt */
26 void WaitForMainInt(){
   pauseMainCLK = 1;
28   while(pauseMainCLK != 0);
}
30
/* Interrupt-Funktion SPI_S */
32 CY_ISR(Interrupt_SPIS){
   SPIMasterS_ReadTxStatus();
34   pauseSPIS = 0;
   return;
36 }

38 /* Warten auf SPI_S Interrupt */
void WaitForSPISInt(){
40   pauseSPIS = 1;
   while(pauseSPIS != 0);
42 }
```

```
44
/* Interrupt-Funktion SPI_R */
46 CY_ISR(Interrupt_SPIR){
    SPIMasterR_ReadTxStatus();
48  pauseSPIR = 0;
    return;
50 }

52 /* Warten auf SPI_R Interrupt */
   void WaitForSPIRInt(){
54  pauseSPIR = 1;
    while(pauseSPIR != 0);
56 }

58 /* Interrupt-Funktion SPI_R */
   CY_ISR(Interrupt_Timer1){
60  ustimer=1;
    return;
62 }


64
/* Warte bestimmte Zeit */
66 void WaitForTime(int zeit){
      ustimer=0;
68  Timer_1_WritePeriod(60*zeit);        // zeit x 1us
    while(ustimer!=1);
70 }


72
//function send data to DAC
74 void sendDataToDAC(float xout) {
      signed int out;
76
      out = (signed int)(xout*2048*1.4); // xout should be not larger than +-1
78
      //Send Signal to DAC
80    SPIMasterS_WriteByte(0x0800 - out);
      WaitForSPISInt();
82    SPIMasterS_WriteByte(0x8800 + out);
      WaitForSPISInt();
84 }

86 //function send data to DAC
   float readDataFromADC(int channel) {
88    float dataFromWater;
      signed int daten[6];
90      int i;

92    Convest_Write(1);          // Start Convest
      WaitForTime(1);
94    SPIMasterR_ClearRxBuffer(); // Clear SPI_R
      SPIMasterS_ClearRxBuffer(); // Clear SPI_S
96    WaitForTime(4);          // Wait for Convest (4us)
      Convest_Write(0);        // Stop Convest
98
```

```
    // Readout Data */
    for(i=0; i<6; i++) {
      SPIMasterR_WriteByte(0x0000);
      WaitForSPIRInt();
      daten[i] = SPIMasterR_ReadRxData();
    }
    // convert data
    if (daten[channel]<32767) dataFromWater=(float)daten[channel]*5/32767;
        else                  dataFromWater= -(65536 - (float)daten[channel])*5/32767;
  return dataFromWater;
}

// send data to PC
void sendToUSB(float aux){
    UART_WriteTxData((signed int)((aux)*40000)>>8);
    UART_WriteTxData((signed int)((aux)*40000)&0x00FF);
}

// make self-calibration for the value of alpha
void selfCalibrate(viod){
  float x=0.1, x_w;
  int i;
  water_factor1=0;
  water_factor2=0;

  for(i=0; i<1000; i++) x=x*(2.0-3.1*x-3.1); //preevaluation
  for(i=0; i<100; i++) {
    x=x*(2.0-3.1*x-3.1);
    sendDataToDAC(x);              //send to DAC
    x_w=readDataFromADC(1);        //read ADC
    WaitForMainInt();
    }
  for(i=0; i<100; i++) {
    x=x*(2.0-3.1*x-3.1);
    sendDataToDAC(x);              //send to DAC
    x_w=readDataFromADC(1);        //read ADC
    if (x_w==0) x_w=0.0000000001;              // to prevent error
    if (x>0) water_factor1=water_factor1+x/x_w; else water_factor2=water_factor2+x/x_w;
    WaitForMainInt();
    }
  sendDataToDAC(0);              //send to DAC
  water_factor1=water_factor1/50;
  water_factor2=water_factor2/50;
}


// make all necessary initializations
void initialize (void) {
  /* Start UART */
  UART_Start();
  /* Starte SPI S */
  Timer_1_Enable();
  Timer_1_Start(); // start 16bit timer
  SPIMasterS_Start();
  /* Starte SPI R */
```

```
154   SPIMasterR_Start();
      /* Starte Timer */
156   Counter_MainCLK_Start();
      /* Starte Interrupt */
158   isr_MainCLK_SetVector(Interrupt_MainCLK);
      isr_Timer1_SetVector(Interrupt_Timer1);
160   isr_Timer1_Enable();
      isr_MainCLK_Enable();
162   isr_SPIS_SetVector(Interrupt_SPIS);
      isr_SPIR_SetVector(Interrupt_SPIR);
164   isr_SPIS_Enable();
      isr_SPIR_Enable();
166   CYGlobalIntEnable;
      /* Reset */ Convest_Write(1);
168   Reset_Write(1);
      WaitForTime(8);
170   Reset_Write(0);
      Convest_Write(0);
172 }

174
/*--------------------------------------*/
176           /*Bifurcation Diagram*/
/*--------------------------------------*/
178
#if ActiveExperiment==0
180
void main()
182 {
      float x = 0.1;
184   float alpha_min=2.9;
      float alpha_max=3.9;
186   float alpha_step=0.005;
      float alpha=alpha_min;
188   float water_factor;
      float x_w=0;
190   unsigned int n=1;
      unsigned short i, uartdata, sender=0;
192
       initialize ();
194
        for (;;)
196     {
        uartdata = UART_GetRxBufferSize(); // Matlab Trigger
198     if(uartdata != 0) sender=1;
        if (sender){
200
        if (n>=500){                    // to make bifurcation diagram
202       n=0;
          x=0.1;
204       alpha=alpha+alpha_step;
          for(i=0; i<10000; i++) x=x*(2.0-alpha*x-alpha); //preevaluation
206       if (alpha>alpha_max) exit(0);
        }
208     n++;
```

```
    sendDataToDAC(x);                   //send to DAC
    WaitForTime(250);                   // wait for rising voltage
    x_w=readDataFromADC(1);             //read ADC
    if (x_w==0) x_w=0.0000000001;                   // to prevent error
    if (x<0) water_factor=0.0792; else water_factor=0.0575;
    sendToUSB(x-x_w*water_factor);          // send to PC via USB
    x=x*(2.0-alpha*x-alpha)-0.05*(x-x_w*water_factor);   //main equation
    if (x>1) x=1;   if (x<-1) x=-1;
    }
  WaitForMainInt();
   }
}

/*-------------------------------------*/
        /*Coupled Oszilators*/
/*-------------------------------------*/
#elif ActiveExperiment==1

void main()
{
  float x = 0.1;
  float xold = 0.1;
  float alpha=3.1;
  float water_factor, xk, xkold;
  float x_w=0.0;
  unsigned short i;
  unsigned short uartdata, sender=0;

   initialize ();
  selfCalibrate ();     //calibrate for water_factor

  for(i=0; i<1000; i++) x=x*(2.0-alpha*x-alpha); //preevaluation
  for (;;)
    {
    uartdata = UART_GetRxBufferSize(); // Matlab Trigger
    if(uartdata != 0) sender=1;
    if (sender){
      sendDataToDAC(x);                 //send to DAC
      x_w=readDataFromADC(1);           //read ADC
      if (x_w==0) x_w=0.0000000001;                 // to prevent error
      if (x<0) water_factor=water_factor2; else water_factor=water_factor1;
      x=x*(2.0-alpha*x-alpha)-0.5*(x-x_w*water_factor);   //main equation
      if (x>1) x=0.1;   if (x<-1) x=-0.1;
      // send to PC via USB
      sendToUSB(x);
          }
    WaitForMainInt();
    }
}

#endif

/* [] END OF FILE */
```

A.2 MatLab Software

A.2.1 Experiment 1 and 3

```
1
% Handles
3 handles = guihandles(gcf);
axes(handles.axes1);
5
% Serielle Verbindung
7 s = start_serial();

9 % Mittellinie
plot([0 1],[0 0], 'k--');
11 grid on;
hold on;
13
% Datenfelder erstellen
15 daten = zeros(1000,1);

17 % Plots erstellen
p = plot(0.001:0.001:1, daten,'b');
19
% Skalierung setzen
21 axis([0 1 -5.5 5.5])

23 % Mainloop
run = true;
25 global number; number = 1;
wert = 1;
27
% Sync ausloesen
29 fwrite(s, number);
fwrite(s, get(handles.popupmenu_filter, 'Value')+9);
31
while(run)
33     tic;

35     % Aktueller Wert erhoehen;
       if wert>=1000
37         wert = 1;
       else
39         wert = wert + 1;
       end
41
       % Messung abrufen
43     wait_response(s,5,2);
       uartdaten = fread(s,2, 'uint8');
45
       % Messung verarbeiten
47
       daten(wert) = uartdaten(1)*256 + uartdaten(2);
49
       if daten(wert)<32767
```

```
51              daten(wert)=daten(wert)/40000;
    else
53              daten(wert) = 65536 - daten(wert);
                daten(wert)=-daten(wert)/40000;
55      end

57      % Plot darstellen
        if mod(wert,20)==0
59          set(p,'Ydata', daten);
            set(handles.text_app, 'string', ['Ap-p: ' num2str(max(daten)-min(daten), '%1.3f') 'V']);
61          set(handles.text_mean, 'string', ['Mean: ' num2str(mean(daten), '%1.3f') 'V']);
            pause(0.0001);
63      end
      % disp(toc)
65      while (toc < 0.001)
            pause(0.00001);
67      end
end
69
% Serielle Verbindung beenden
71 stop_serial(s);
```

A.2.2 Experiment 2

```
2  clear all
   % Handles
4  handles = guihandles(gcf);
   axes(handles.axes1);
6
   % Serielle Verbindung
8  s = start_serial();

10 % Mittellinie
   plot([0 1],[0 0], 'k--');
12 grid on;
   hold on;
14
   % Datenfelder erstellen
16 daten = zeros(1000,1);

18 % Plots erstellen
   p = plot(0.001:0.001:1, daten,'b');
20
   % Skalierung setzen
22 axis([0 1 -5.5 5.5])

24 %MicroController Loop Trigger
   fwrite(s, 1);
26 fwrite(s, get(handles.popupmenu_filter, 'Value')+9);

28 % Mainloop
```

```
run = true;
global number; number = 1;
wert = 1;
alpha_start=2.9;
alpha_end=3.9;
alpha=alpha_start;
alpha_step=0.005;
alpha_vector=(0:alpha_step:round(alpha_end/alpha_step)-1);
period=1;
max_periods=50;
period_vector=zeros(round(alpha_end/alpha_step),1);
BifurcationMap=zeros(max_periods,round(alpha_end/alpha_step));
Chaos=zeros(round(alpha_end/alpha_step),1);

while(run)
    tic;


    % Aktueller Wert erhoehen;
    if wert>=500
        wert = 1;
        alpha=alpha+alpha_step;
        period=1;

    else
        wert = wert + 1;
    end

    if alpha>alpha_end

        break

    end

    % Messung abrufen
    wait_response(s,5,2);
    uartdaten = fread(s,2, 'uint8');

    % Messung verarbeiten


    daten(wert) = uartdaten(1)*256 + uartdaten(2);

    if daten(wert)<32767
         daten(wert)=daten(wert)/40000;
    else
        daten(wert) = 65536 - daten(wert);
        daten(wert)=-daten(wert)/40000;
    end




  %-----------------------------------------------------------
```

```
84
   if wert==200
86
       alpha_vector(round(alpha/alpha_step))=alpha;
88
            for i=1:50
90              BifurcationMap(i,round(alpha/alpha_step))=daten(wert-max_periods+i-1);
            end
92
        period_vector(round(alpha/alpha_step))=period;
94
   end
96
    %-------------------------------------------------------------
98
100
      % Plot darstellen
102    if mod(wert,20)==0
           set(p,'Ydata', daten);
104        set(handles.text_app, 'string', ['Alpha: ' num2str(alpha, '%1.3f') 'V']);
           set(handles.text_mean, 'string', ['Mean: ' num2str(mean(daten), '%1.3f') 'V']);
106        pause(0.0001);
       end
108    % disp(toc)
       while (toc < 0.001)
110        pause(0.00001);
       end
112
end
114
BifurcationToDat(BifurcationMap);
116 %end PSoC sequence
 fwrite(s, 0);
118
% Serielle Verbindung beenden
120 stop_serial(s);

122 %Plot Bifurcation Diagram
BifurcationPloter
```

Bibliography

[1] **Jacques Cousteau**. *The Ocean World*. Harry N. Abrams, 1985

[2] Census of Marine Life *http://www.coml.org/*

[3] **A. A. Archer**,Economics of Off-shore Exploration and Production of Solid Minerals on the Continental Shelf 1. 1973

[4] **Henry Fountain**, ABE, Pioneering Robotic Undersea Explorer, Is Dead at 16. *The New York Times* March 15.03.2010 *http://www.nytimes.com/2010/03/16/science/16sub.html*

[5] **Peter Brewer**, Swarming mini-subs to change undersea science. *Canberra Times* 31.07.2004 p. 5

[6] **t.Bean et al**, AUV Cooperative Operations using Acoustic Communication and Navigation, *IEEE Journal of Oceanic Engineering* Sept. 2007

[7] **Eduardo R. B. Marques et al**, AUV Control and Communication using Underwater Acoustic Networks, *Oceans*, 2007

[8] **Heather Brundage**,Designing a Wireless Underwater Optical Communication System, 2010

[9] **Dirk Speneberg, Christoph Waldmann, Richard Babb**, Exploration of Underwater Structures with Cooperative Heterogeneous Robots. *Oceans-Europe* 2005

[10] **T. Dipper, K. Gebhardt, S. Kernbach, G. von der Emde**, Investigating the behaviour of weakly electric fish with a Fish Avatar. 2011

[11] **Malcolm A. MacIver, Ebraheem Fontaine, Joel W. Burdick**, Designing Future Underwater Vehicles: Principles and Mechanisms of the Weakly Electric Fish, *IEEE Journal Of Oceanic Engineering*, Vol.29, No.3, July 2004

[12] **Serge Kernbach, Tobias Dipper**, Potential-Field-Coupled Oscillators for Coordination of Collective Behavior in Underwater Robotics, *IEEE Transactions on Robotics*

[13] Angels Project *http://www.theangelsproject.eu/*

[14] CoCoRo Project *http://cocoro.uni-graz.at/*

[15] **N.B.Tufillaro,T.Abbott,andJ.Reilly** *An Experimantal Approach to Nonlinear Dynamics and Chaos*. AddisonWesley, 1992.

[16] **Viktor Avrutin** *University lecture: Introduction to Chaos Theory* Universität Stuttgart 2011

[17] **Hassan Khalil**. *Nonlinear Systems*. Prentice Hall, 2002

[18] **Steven Strogatz**. *Nonlinear Dynamics and Chaos*. West View Press, 2000

[19] **John David Jackson** *Classical Electrodynamics*. Wiley, 1975

[20] Cypress Perform PSoC®5 *http://www.cypress.com/?id=2233*

[21] PSoC Creator Visual Embedded Design Tool *http://www.cypress.com/?docID=21310*

[22] Mathworks MatLab *http://www.mathworks.com/products/matlab/*

[23] **Michael Schanz et. al** Dynamic Task Assignment in a Team of Agents *Autonome Mobile Systeme 2005*

All links were last followed on 21.12.2012.

Declaration

All the work contained within this thesis, except where otherwise acknowledged, was solely the effort of the author. At no stage was any collaboration entered into with any other party.

(Everardo González Ávalos)